Conical diffraction in optically active crystals

M R Jeffrey

H H Wills Physics Laboratory, Tyndall Avenue, Bristol BS8 1TL

mike.murrill@bristol.ac.uk

Abstract. Light passing along the optic axis of a slab of transparent biaxial crystal is considered in the presence of optical activity. The dominant feature in the intensity, described analytically here, is a bright cone inside the crystal, refracting into a bright horn at the exit face, due to a divergence of the intensity of geometric rays. This divergence is removed by diffraction, which introduces recently discovered asymptotic features, including Airy rings across the caustic horn, and a spun cusp catastrophe. Here we concentrate on the region close to the focal image plane, and a different set of fringes previously seen in experiments by Schell and Bloembergen. The intensity pattern here depends dramatically on the polarisation of the incident beam, and we present a simple analytic formula for the intensity when the incident beam is linearly polarised.

1. Introduction

Recent advances in the theory of conical diffraction have unveiled a subtle interplay between geometrical optics and wave diffraction. Hamilton's study of Fresnel's wave surface in 1832 [1] led him to predict that a single ray of light, incident upon a slab of biaxial crystal along its optic axis, should refract into an infinite number of rays forming the surface of a hollow cone, a phenomenon he called internal conical refraction. The cone would refract into a hollow cylinder at the crystal exit face, visible as a bright ring on a screen behind the crystal. Although this striking phenomenon was quickly confirmed by experiment [2], it was not until the end of the decade that better resolution revealed two concentric rings separated by a "coal black sliver" [3, 4]. Hamilton himself appreciated that his idealised ray theory of conical refraction would not be physically accurate, but it took until 1905 for Voigt to explain the importance of the spread of wave directions in a physical beam of light [5], beginning a wave theory of conical diffraction that would take another century to complete [3, 6, 7].

Two essential principles led to a full understanding: firstly, the simplification of paraxiality, where deflection angles from the optic axis are small; and secondly, that although much of the phenomenon can be understood in terms of geometrical rays, a complete description requires polarised waves. This is particularly evident in the case of chiral conical diffraction, in which a beam of light, passing along the optic axis of a slab of biaxial optically active crystal, emerges as a bright caustic horn. That optically active crystals would still exhibit something approximating conical refraction has long been known [8], but the definitive wave theory was only formulated in 2002 [9], and the dominant features found more recently [10].

Here we present new aspects of the theory of chiral conical diffraction that demonstrate the above principles. In section 2 we develop the geometrical optics and relate the modern view to Hamilton's discovery. In section 3 we consider the intensity of light rays passing through an optically active crystal, relating them to the caustic horn and spun cusp that form beyond the crystal, identified in [10].

In section 4 we consider the spiral intensity pattern that dominated 20th century interest in the phenomenon [8, 9, 11, 12], caused by the diffraction of a linearly polarised light beam passing through an optically active crystal, and we obtain a simple analytic formula for the intensity.

A biaxial crystal is characterised by three principal refractive indices $n_1<n_2<n_3$. Hamilton's cone has the optic axis as one of its generators, perpendicular to which its cross-section is circular, with cone semi-angle

$$A = \frac{1}{n_2}\sqrt{(n_2 - n_1)(n_3 - n_2)}. \tag{1.1}$$

Paraxial analysis is appropriate because this angle is typically small (0.93° for aragonite). Optical activity can arise either from macroscopic chirality of the crystal, or from the Faraday effect. In either case the effect is specified by a single parameter: the optical rotary power Γ.

2. The paraxial theory of chiral conical refraction

For a plane wave with vacuum wavenumber k_0, we expand in terms of the small part of the wavevector transverse to the optic axis, $\mathbf{k}_\perp = (k_x, k_y)$. We define a crystal wavenumber $k=n_2k_0$, and exploit the transversality of the electrical displacement vector **D**. From Maxwell's equations, **D** satisfies the eigenequation

$$\frac{1}{n^2}\mathbf{D}(\mathbf{k}_\perp) = \mathbf{M}(\mathbf{k}_\perp)\cdot\mathbf{D}(\mathbf{k}_\perp) \tag{2.1}$$

where, paraxially,

$$\mathbf{M}(\mathbf{k}_\perp) \approx \frac{1}{n_2^2}\left(\mathbf{1} - \frac{1}{k}\begin{pmatrix} Ak_x & Ak_y - i\Gamma \\ Ak_y + i\Gamma & -Ak_x \end{pmatrix}\right), \tag{2.2}$$

with eigenvalues

$$\frac{1}{n^2} \approx \frac{1}{n_2^2}\left(1 \pm \frac{1}{k}\sqrt{A^2k_\perp^2 + \Gamma^2}\right). \tag{2.3}$$

Let position in space be denoted $\mathbf{r} = (\mathbf{r}_\perp, z)$, in terms of the transverse position $\mathbf{r}_\perp$, and the distance z along the optic axis measured from the sharpest focus of the incident beam. It is convenient to define dimensionless variables for a crystal slab of length l and a beam of width w. Transverse position $\boldsymbol{\rho}$ is measured in units of the beam width, with corresponding wavevector $\boldsymbol{\kappa}$, and propagation distance ζ is measured from the focal image plane along the optic axis in units of kw^2:

$$\boldsymbol{\rho} = \mathbf{r}_\perp / w, \qquad \boldsymbol{\kappa} = w\mathbf{k}_\perp, \qquad \zeta = \left(l + n_2(z - l)\right)\Big/ kw^2. \tag{2.4}$$

Birefringence and chirality can be represented in terms of two phases: $\rho_0=Al/w$, which is the radius of Hamilton's cone at the exit face in units of w, or the phase difference accumulated in the crystal by two plane eigenwaves travelling at a deflection angle $1/k_0w$ from the optic axis; and γ, which is the phase accumulated in the crystal by a circularly polarised wave travelling along the optic axis.

The direction dependent refractive indices for two paraxial plane waves can then be written as

$$n(\kappa) \approx n_2\left(1 \pm \tfrac{1}{kl}\sqrt{\rho_0^2\kappa^2 + \gamma^2}\right). \tag{2.5}$$

In the absence of chirality this describes the diabolical point at $\kappa=0$, but the degeneracy is removed by a non-zero γ. The optical path length of a ray exiting the crystal is then

$$\Phi(\boldsymbol{\kappa}) = \boldsymbol{\rho}\cdot\boldsymbol{\kappa} - \tfrac{1}{2}\zeta\kappa^2 \mp \sqrt{\rho_0^2\kappa^2 + \gamma^2}\,. \tag{2.6}$$

The wave surface $\boldsymbol{\rho}\cdot\boldsymbol{\kappa}-\Phi(\boldsymbol{\kappa})$ is a phase contour in $\boldsymbol{\kappa}$-space, whose vector normals are the rays:

$$\boldsymbol{\rho}(\boldsymbol{\kappa})=\nabla_{\boldsymbol{\kappa}}\left(\boldsymbol{\rho}\cdot\boldsymbol{\kappa}-\Phi(\boldsymbol{\kappa})\right)=\left(\zeta\pm\rho_0^2\Big/\sqrt{\rho_0^2\kappa^2+\gamma^2}\right)\boldsymbol{\kappa}. \tag{2.7}$$

For values of ζ corresponding to positions inside the crystal, this is the "virtual wave" surface, whose normals are the projection of the external rays back inside the crystal. Hamilton was aware, and credited to Cauchy the discovery, that the wave surface is related to a dual surface often called the ray surface, in this case $\boldsymbol{\rho}\cdot\boldsymbol{\kappa}-\Theta(\boldsymbol{\kappa})$, defined by the property that its normals are the wavevectors

$$\boldsymbol{\kappa}(\boldsymbol{\rho})=\nabla_{\boldsymbol{\rho}}\left(\boldsymbol{\rho}\cdot\boldsymbol{\kappa}-\Theta(\boldsymbol{\kappa})\right)=\left(\rho\mp\rho_0^2\kappa\Big/\sqrt{\rho_0^2\kappa^2+\gamma^2}\right)\frac{\boldsymbol{\rho}}{\rho\zeta}. \tag{2.8}$$

The duality of the surfaces can be expressed by a Legendre transform,

$$\nabla_{\boldsymbol{\rho}}\left(\boldsymbol{\rho}\cdot\boldsymbol{\kappa}-\Theta(\boldsymbol{\rho})\right)=\left[\nabla_{\boldsymbol{\kappa}}\left(\boldsymbol{\rho}\cdot\boldsymbol{\kappa}-\Phi(\boldsymbol{\kappa})\right)\right]^{-1} \tag{2.9}$$

where the '-1' denotes the inverse function.

In the absence of chirality we can draw a useful analogy to Hamilton's investigation of the true wave surface inside the crystal [1, 13]. Corresponding to the conical point of the wave surface at $\kappa=0$ responsible for internal conical refraction, there is a circle of contact on the ray surface at $\rho=\rho_0$. Conversely, the circle of contact on the wave surface at $\kappa=\rho_0/\zeta$, corresponds to the conical point of the ray surface at $\rho=0$ noted in Hamilton's original investigation [1]. (The circle of contact is the unique ring of points on the curved surface that can be touched by a single tangent plane).

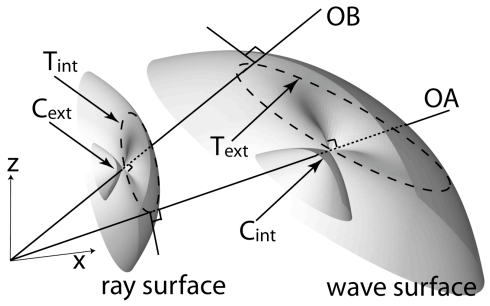

Figure 1. Geometry of conical refraction (nonchiral). The picture shows the correspondence between: the optic axis OA, conical point C_{int} of the wave surface, and circle of contact T_{int} on the ray surface; and between: the binormal OB, circle of contact T_{ext} on the wave surface, and conical point C_{ext} of the ray surface. The paraxial portions of the surfaces shown are enlarged and angles are exaggerated for clarity.

In the presence of chirality these degeneracies disappear, but are replaced by a rich singular structure examined in the next section. In particular the wave surface is fourth order, that is, the ray directions κ are the real roots of a quartic obtained from (2.8).

3. Geometrical optics in the crystal

For observations it is sufficient to consider, as above, only the total optical path of rays once they have exited the crystal, since any lens placed beyond the exit face images either the light intensity outside the crystal ($\zeta>l/kw^2$), or the virtual image field intensity found by projecting these rays back inside the crystal ($\zeta<l/kw^2$). Given the striking image intensity of chiral conical refraction, however, it is interesting to consider also the ray intensity inside the crystal that causes it.

We first summarize the intensity of the image field found in [10]. In terms of the real solutions $\kappa_n(\rho)$ of (2.8), and a circularly symmetric incident beam profile $a(\kappa)$, this is given by

$$I(\rho,\zeta)=\frac{1}{2}\sum_n\left\{\left|a(\kappa)\right|^2\frac{\kappa}{\rho}\left(\zeta+\left(\frac{\gamma}{\rho_0^2}\right)^2\left(\frac{\rho}{\kappa}-\zeta\right)^3\right)^{-1}\right\}_{\kappa=\kappa_n(\rho)}. \tag{3.1}$$

This geometrical optics formula diverges where axial focussing occurs, on a line along the optic axis,

$$\rho = 0, \quad \zeta \le \rho_0^2 \big/ \gamma \equiv \zeta_{\text{cusp}}, \tag{3.2}$$

which threads a caustic surface of revolution,

$$\left(\rho/\rho_0\right)^{2/3} + \left(\zeta/\zeta_{\text{cusp}}\right)^{2/3} = 1, \tag{3.3}$$

the caustic "horn", whose mouth is in the focal plane ζ=0 with radius $\rho=\rho_0$, and whose apex is a spun cusp at $\zeta=\zeta_{\text{cusp}}$. This can be seen in figures 2(e),(f).

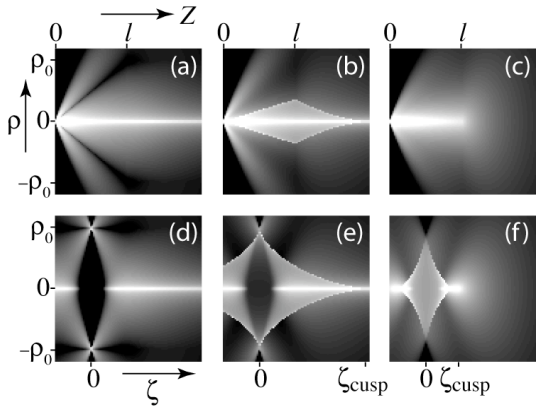

Figure 2. (a-c) Log of ray intensity inside, $Z<l$, and outside, $Z>l$, the crystal in the $r_\perp$,Z or ρ,ζ plane, for: (a) $A^2/G\to\infty$ (nonchiral); (b) A^2/G=3, showing the caustic cone and horn; (c) A^2/G=5/4 (strong chiral). (d-e) Log of geometrical image intensity corresponding to (a-c), showing the intensity of virtual rays projected back into the crystal.

Inside the crystal it is more convenient to define new dimensionless variables: the deflection vector $\boldsymbol{\theta}$ of a ray, and corresponding deflection wavevector $\mathbf{P}$, and suitable optical rotary power variable G:

$$\boldsymbol{\theta} = \mathbf{r}_\perp \big/ z, \qquad \mathbf{P} = \mathbf{k}_\perp \big/ k, \qquad G = \Gamma \big/ k, \tag{3.4}$$

The optical path length in the crystal becomes

$$\Phi\left(\mathbf{P}\right) = kz\left(\boldsymbol{\theta}\cdot\mathbf{P} - \tfrac{1}{2}P^2 \mp \sqrt{A^2P^2 + G^2}\right), \tag{3.5}$$

and the intensity,

$$I\left(\theta, z\right) = \tfrac{1}{2}\left(\frac{z}{kw^2}\right)^{-2} \sum_n \left\{ \left|a\left(P\right)\right|^2 \frac{P}{\theta}\left(1 + \left(\frac{G}{A^2}\right)^2 \left(\frac{\theta}{P} - 1\right)^3\right)^{-1} \right\}_{P=P_n(\theta)}. \tag{3.6}$$

where the wavenumbers $P_n(\theta)$ are the real solutions of a quartic equation:

$$\left(\theta - P\right)^2 \left(A^2P^2 + G^2\right) - A^4P^2 = 0. \tag{3.7}$$

The intensity again diverges along θ=0 due to axial focussing, and along a caustic cone,

$$\left(\theta/A\right)^{2/3} + \left(G/A^2\right)^{2/3} = 1, \tag{3.8}$$

first identified by Voigt [8], caused by a ring of inflection points in the wave surface surrounding the conical point. The rays forming this caustic cone refract out of the crystal to form the image caustic (3.3), as is evident from the coincidence of the interior caustic cone and exterior caustic horn at the exit face $z=kw^2\zeta=l$, where $\theta=\rho w/l$, shown in figure 2(b).

4. Diffraction Asymptotics

The paraxially exact wave theory is achieved by representing an incident beam of monochromatic light by a superposition of plane waves,

$$\mathbf{D}\left(\boldsymbol{\rho},\zeta\right) = \tfrac{1}{2\pi}\iint \mathrm{d}\boldsymbol{\kappa} \exp\left(\mathrm{i}\boldsymbol{\rho}\cdot\boldsymbol{\kappa} - \mathrm{i}\mathbf{F}\left(\boldsymbol{\kappa}\right)\right) a\left(\kappa\right)\mathbf{d}_0, \tag{4.1}$$

for a circularly symmetric incident beam profile $a(\kappa)$ with polarisation state $\mathbf{d}_0$, evolving along the optic axis according to the unitary operator $e^{-i\mathbf{F}}$, where

$$\mathbf{F}(\boldsymbol{\kappa})=\tfrac{1}{2}\kappa^2\zeta\mathbf{1}+\mathbf{S}\cdot(\rho_0\boldsymbol{\kappa},\gamma),\qquad \mathbf{S}=(\sigma_3,\sigma_1,\sigma_2), \tag{4.2}$$

where $\boldsymbol{\sigma}_n$ are the Pauli matrices. This leads to plane waves

$$\mathbf{D}(\boldsymbol{\rho},\zeta)=\left[B_0(\rho,\zeta)\mathbf{1}+\mathbf{S}\cdot\left\{\frac{\boldsymbol{\rho}}{\rho}B_1(\rho,\zeta),B_2(\rho,\zeta)\right\}\right]\mathbf{d}_0, \tag{4.3}$$

in terms of three diffraction integrals [9, 10]:

$$B_0(\rho,\zeta)=\int_0^\infty \mathrm{d}\kappa\kappa a(\kappa)\exp\left(-\tfrac{1}{2}\mathrm{i}\kappa^2\zeta\right)\mathrm{J}_0(\rho\kappa)\cos\sqrt{\rho_0^2\kappa^2+\gamma^2}$$

$$B_1(\rho,\zeta)=\frac{\rho_0}{\gamma}\frac{\partial^2}{\partial\rho\partial\gamma}B_0(\rho,\zeta),\qquad B_2(\rho,\zeta)=\mathrm{i}\frac{\partial}{\partial\gamma}B_0(\rho,\zeta) \tag{4.4}$$

The intensity is given by

$$I(\boldsymbol{\rho},\zeta)=\left|\mathbf{D}(\boldsymbol{\rho},\zeta)\cdot\mathbf{D}(\boldsymbol{\rho},\zeta)^*\right|^2 \tag{4.5}$$

For an unpolarised incident beam this was first given in [9]:

$$I_{\text{unpol}}=|B_0|^2+|B_1|^2+|B_2|^2, \tag{4.6}$$

where the intensity for linear and circular polarisation were also given. Here we will be concerned with a linearly polarised incident beam $\mathbf{d}_0=(\cos\chi,\sin\chi)$, for which the intensity becomes

$$I_\chi=I_{\text{unpol}}+2\,\mathrm{Re}\left[B_0^*B_1\right]\cos\left(2\chi-\phi_{\boldsymbol{\rho}}\right)+2\,\mathrm{Im}\left[B_1^*B_2\right]\sin\left(2\chi-\phi_{\boldsymbol{\rho}}\right). \tag{4.7}$$

The asymptotics of the integrals (4.4) was studied in [10], particularly near the caustic (3.3) and cusp (3.2). The central result is the expression, (correcting a missing $\sqrt{\kappa_n}$ in the numerator from [10]),

$$B_0(\rho,\zeta)\approx\frac{1}{2\sqrt{\rho}}\sum_n\sqrt{\frac{\kappa_n}{\left|\Phi''(\kappa_n)\right|}}a(\kappa_n)\exp\left\{\mathrm{i}\left(\tfrac{1}{2}\left(\arg\kappa_n-\arg\Phi''(\kappa_n)\right)+\Phi(\kappa_n)\right)\right\}. \tag{4.8}$$

Near the focal image plane, i.e. for $\zeta<<\rho_0^2/\gamma$, this simplifies significantly with the introduction of the scaled position vector $\mathbf{u}$, and accompanying variable $v>0$, defined such that

$$\mathbf{u}=\boldsymbol{\rho}/\rho_0,\qquad u^2+v^2=1. \tag{4.9}$$

Far from the caustic, that is for $u<<v\approx1$, the diffraction integrals can then be written:

$$\begin{Bmatrix}B_0(\rho,\zeta)\\B_1(\rho,\zeta)\\B_2(\rho,\zeta)\end{Bmatrix}\approx\frac{\gamma}{\rho_0^2v}\exp\left(\frac{\mathrm{i}\zeta}{2\rho_0^2v^2}\right)a\left(\frac{\gamma u}{\rho_0 v}\right)\begin{Bmatrix}-\sin\gamma v\\-u\sin\gamma v\\\mathrm{i}v\cos\gamma v\end{Bmatrix}. \tag{4.10}$$

The intensity can then be written simply as

$$I_\chi(u)\approx\left(\frac{\gamma}{\rho_0^2}\right)^2\left|a\left(\frac{\gamma u}{\rho_0 v}\right)\right|^2\frac{1-u^2\cos(2\gamma v)+2u\sin(\gamma v)\sin(\gamma v+\phi_{\mathbf{u}}-2\chi)}{v^4}. \tag{4.11}$$

Figure 3 shows that this ζ-independent expression correctly captures the intensity pattern given by the exact integrals (4.4). This simulation agrees qualitatively with the experimental figure 5B from [11], (previously reproduced in [9] along with a simulation using the exact integrals (4.4)), which contains the only detailed observations of chiral conical diffraction known to us.

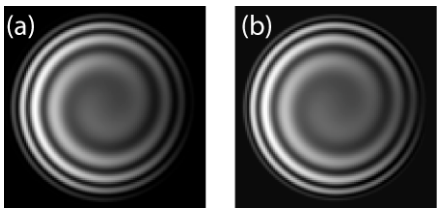

Figure 3. Intensity in the focal image plane for a vertically polarised incident beam, for $\rho_0=-\gamma=20$. (a) is calculated from the exact formulae (4.4) and (4.7). (b) is calculated from the approximation (4.11).

5. Concluding remarks

The surprising singular nature of chiral conical diffraction can be explained by considering geometrical rays, derived by considering the form of the wave surface for light leaving the crystal. The dominant features – a caustic surface and a spun cusp – have not yet been observed. As well as softening the geometric singularities, diffraction adds rich structure, one element of which has been observed, namely a set of fringes near the focal image plane. For these, the theoretical and experimental diffraction patterns for a linearly polarised incident beam are in good agreement.

Two further intriguing extensions of Hamilton's discovery remain: to introduce dichroism (anisotropic absorption), and nonlinearity. Dichroism fundamentally alters the mathematical structure of the problem, reintroducing the degeneracy, but splitting the optic axis into a pair of singular axes. We are presently exploring this new phenomenon, and will report the results later. Nonlinearity is also the subject of current study, see [14].

Acknowledgements

I thank Professor Sir Michael Berry for his part in this work. This research is supported by the Royal Society.

References

[1] Hamilton, W. R.,1837, Third Supplement to an Essay on the Theory of Systems of Rays *Trans. Royal Irish Acad.* **17**, 1-144.

[2] Lloyd, H.,1837, On the phenomena presented by light in its passage along the axes of biaxial crystals *Trans. R. Ir. Acad.* **17**, 145-158.

[3] Berry, M. V., Jeffrey, M. R. & Lunney, J. G.,2006, Conical diffraction: observations and theory *Proc. R. Soc. A* **462**, 1629-1642.

[4] Poggendorff, J. C.,1839, Ueber die konische Refraction *Pogg. Ann.* **48**, 461-462.

[5] Voigt, W.,1905, Bemerkung zur Theorie der konischen Refraktion *Phys. Z.* **6**, 672-673.

[6] Berry, M. V. & Jeffrey, M. R.,2006, Conical diffraction: Hamilton's diabolical point at the heart of crystal optics *submitted to Progress in Optics* **50**.

[7] Belskii, A. M. & Khapalyuk, A. P.,1978, Internal conical refraction of bounded light beams in biaxial crystals *Opt. Spectrosc. (USSR)* **44**, 436-439.

[8] Voigt, W.,1905, Theoretisches und Experimentalles zur Aufklaerung des optischen Verhaltens aktiver Kristalle *Ann. Phys.* **18**, 645-694.

[9] Belsky, A. M. & Stepanov, M. A.,2002, Internal conical refraction of light beams in biaxial gyrotropic crystals *Opt. Commun.* **204**, 1-6.

[10] Berry, M. V. & Jeffrey, M. R.,2006, Chiral conical diffraction *J. Opt. A* **8**, 363-372.

[11] Schell, A. J. & Bloembergen, N.,1978, Laser studies of internal conical diffraction. II. Intensity patterns in an optically active crystal, α-iodic acid *J.Opt.Soc.Amer.* **68**, 1098-1106.

[12] Portigal, D. L. & Burstein, E.,1972, Effect of Optical Activity or Faraday Rotation on Internal Conical Refraction *J.Opt.Soc.Amer.* **62**, 859-864.

[13] Landau, L. D., Lifshitz, E. M. & Pitaevskii, L. P.,1984, *Electrodynamics of Continuous Media* (Pergamon, Oxford).

[14] Indik, R. A. & Newell, A. C.,2006, Conical refraction and nonlinearity *submitted to Optics Express*.